DALTON
FULL PAPER

How the α-hydroxymethylserine residue stabilizes oligopeptide complexes with nickel(II) and copper(II) ions

Piotr Młynarz,[a] Nicola Gaggelli,[b] Jarosław Panek,[a] Marcin Stasiak,[c] Gianni Valensin,[b] Teresa Kowalik-Jankowska,[a] Mirosław L. Leplawy,[c] Zdzisław Latajka[a] and Henryk Kozłowski*[a]

[a] *Faculty of Chemistry, University of Wrocław, F.Joliot-Curie 14, 50-383 Wroław, Poland. E-mail: henrykoz@wchuwr.chem.uni.wroc.pl*
[b] *Dipartimento di Chimica, Universita di Siena, Via Aldo Moro, 53100 Siena, Italy*
[c] *Institute of Organic Chemistry, Technical University, 90-924 Łódz, Poland*

Received 26th November 1999, Accepted 3rd February 2000
Published on the Web 13th March 2000

Potentiometric, spectroscopic and theoretical studies have shown that the α-hydroxymethylserine (HmS) residue is a very specific amino acid residue when inserted into a peptide sequence. The theoretical calculations as well as evaluated deprotonation microconstants indicated that in the HmS-HmS-His tripeptide the N-terminal ammonium group is more acidic than the imidazole nitrogen. The hydrogen bond formation between the N-terminal amino group and imidazole nitrogen stabilizes the cyclic conformation of the metal-free peptide. The unusual gain in the 4N complex stability in the copper(II) and nickel(II) complexes with HmS-HmS-His ligands seems to derive from the enhancement of the π-electron contribution to the metal–amide nitrogen bond.

Our recent works have shown that α-hydroxymethylserine (HmS), a non-proteinaceous amino acid, is very effective in enhancing the metal binding ability of oligopeptide ligands when inserted into their sequence.[1–4] The insertion of two HmS residues into the peptide sequence with a third His residue leads to the most effective albumin-like chelator.[3] This latter finding has inspired us to perform systematic potentiometric, spectroscopic (including detailed NMR) and theoretical studies in order to evaluate the possible effect of the side chain interactions, which in the case of hydrophobic amino acids[5] or Arg residues[6] were assumed to be critical for the complex stability. The other reason for the high stability constants of metal(II) complexes with peptides having HmS residues inside their sequences could be the low value of the protonation constant of the HmS amino group. This, relatively acidic character of the HmS ammonium group derives from the strong electron withdrawing ability of two hydroxymethyl moieties placed at the α-carbon and as a result it affects the electron density within the peptide bond. The more acidic amide nitrogen is deprotonated easier and bound by metal ions. These two possible causes of the dramatic stability gain observed for HmS peptides were checked in this study.

Experimental

NMR measurements

NMR experiments were carried out at 14.1 T (Bruker Avance 600 MHz) at controlled temperature (±0.1 K). Solutions were made in deuterium oxide (99.95%, Merck), adjusted in pH with either DCl or NaOD and carefully deoxygenated. Chemical shifts were referenced to internal [$^2H_4$]-TSP (trimethylsilylpropanesulfonic acid sodium salt). The NMR spectra were obtained at concentration 5 mM for both ligands and for the complexes in the molar ratio 1:1 of H-HmS-HmS-His-OH:Ni^{II} at pD 7.4 and 1.15:1 H-HmS-HmS-His-NH_2:Ni^{II} at pD 7.3.

TOCSY[7] experiments were acquired with total spin-locking time of 75 ms using a MLEV-17 mixing sequence. Rotating frame Overhauser enhancement spectroscopy (ROESY)[8] was performed at a mixing time of 300 ms with the r.f. strength for the spin lock field held at values lower than 3.5 kHz. NOESY spectra were acquired with standard acquisition parameters. TOCSY, ROESY and NOESY spectra were recorded in the phase-sensitive mode and with water suppression. Spin–lattice relaxation rates were measured with inversion recovery pulse sequences and calculated by exponential regression analysis of the recovery curves of longitudinal magnetization components.

Potentiometric measurements

Stability constants for proton and nickel(II) complexes were calculated from titration curves carried out at 25 °C using a total volume of 1.5 cm^3. Alkali was added from a 0.250 cm^3 micrometer syringe which was calibrated by both weight titration and the titration of standard materials. Ligand concentration was 2×10^{-3} mol dm^{-3} and the metal-to-ligand ratios were 1:1 and 1:1.5. The pH-metric titrations were performed at 25 °C in 0.1 mol dm^{-3} KNO_3 on a MOLSPIN pH-meter system using a Russel CMAW 711 semi-micro combined electrode calibrated in hydrogen ion concentrations using HNO_3.[9] Three titrations were performed for each molar ratio, and the SUPERQUAD computer program was used for stability constant calculations.[10] Standard deviations quoted were computed by SUPERQUAD, and refer to random errors only. They are, however, a good indication of the importance of a particular species in the equilibrium.

Spectroscopic studies

Absorption spectra were recorded on a Beckman DU 650 spectrophotometer, circular dichroism (CD) spectra on a JASCO J 720 spectropolarimeter in the 850–250 nm range. Metal concentration in CD and UV-VIS spectroscopic measurements was adjusted to 3×10^{-3} mol dm^{-3} and the metal to ligand ratio was 1:1. The spectroscopic parameters were obtained at the maximum concentration of the particular species from the potentiometric calculations.

Combined spectrophotometric and pH-metric determination of stability constants of nickel(II) complexes

Owing to very slow co-ordination equilibria in the Ni^{II}-H-HmS-HmS-His-NH_2 systems the calculations based on the potentiometric data were very inaccurate. To evaluate the stability constant of the major complex the spectroscopic method was used.

Stock solutions containing 1.4 mM peptide (H-HmS-HmS-His-NH_2), 1.2 mM $Ni(NO_3)_2$ and 0.1 M KNO_3 were acidified with HNO_3 to pH 2.8. Samples were stored under nitrogen. Single portions of 0.1 M NaOH were added under nitrogen to individual samples of stock solutions, and resulting mixtures were monitored by the absorption band at 416 nm until equilibrium was achieved. Spectra of equilibrated samples were recorded and the final pH values were measured. The absorption band at 416 nm was used as a measure of concentration of the $NiH_{-2}L$ (4N) complex at a given pH, assuming that the average value of the absorption observed for the samples at the pH range 6–9 corresponds to 100% of the complex.

Peptide synthesis

The peptides H-HmS-HmS-His-OH and H-HmS-HmS-His-NH_2 were prepared using optimized methodology for incorporation of HmS into the peptide chain.[11,12] H-HmS-HmS-His-OH was synthesized with 2-chlorotrityl chloride resin (Novabiochem) loaded with Fmoc-His(Boc)-OH.[13] FAB-MS (*m*/*z*): 390 $(MH)^+$, 412 $(MNa)^+$ and 428 $(MK)^+$; calc. for $C_{14}H_{23}N_5O_8$ 389. H-HmS-HmS-His-NH_2 was synthesized starting with N-deprotected dipeptide H-HmS(Ipr)-His(Boc)-NH_2 (Ipr = *O*,*O*-isopropylidene protective group)[4] which was coupled with Boc-HmS(Ipr)-OH in the presence of HATU (*O*-(7-azabenzotriazol-1-yl)-*N*,*N*,*N*′,*N*′-tetramethyluronium hexafluorophosphate). FAB-MS (*m*/*z*): 389 $(MH)^+$, 411 $(MNa)^+$ and 427 $(MK)^+$; calc. for $C_{14}H_{24}N_6O_7$ 388.

Theoretical calculations

Theoretical calculations for selected ligand molecules have been performed in order to obtain additional information about complexing abilities of considered species (*i.e.* H-Gly-Gly-His-OH and H-Hms-Hms-His-OH neutral molecules). Structures have been optimized using a semiempirical AM1 model, and the most stable conformers further refined at the density-functional *ab initio* level (B3LYP/6-31G) with solvent effects included *via* the PCM model of Miertus and Tomasi[14] with relative permittivity $\varepsilon = 78.39$. Charge distribution has been computed by Natural Bond Orbital[15] (NBO) analysis. The calculations were performed with the GAUSSIAN 94[16] program.

Results and discussion

Insertion of two HmS residues into the X-X-His sequence results in a very distinct gain of the stability of the peptide complexes with copper(II) ions.[3] The observed increase in the stability was of several orders of magnitude when compared to the simple Gly-Gly-His ligand and it is a common feature of oligopeptides in which regular amino acids are substituted by the HmS residue(s).[1–4]

Potentiometric and spectroscopic data obtained in this work for Ni^{II} with H-HmS-HmS-His-OH and H-HmS-HmS-His-NH_2 systems indicate the formation of a major planar species $NiH_{-2}L$ above pH 4 (Table 1). The stability of the $NiH_{-2}L$ complex is much higher than that found for the other Ni^{II}–X-Y-His peptide (Table 2a). Similarly to the copper(II) complexes the differences in the stability constants are very distinct, up to 2–3 orders of magnitude.

The gain in stability constant of the $NiH_{-2}L$ complex with strongly hydrophobic Val-Ile-His-Asn peptide having identical, albumin-like binding pattern was assumed to derive from the hydrophobic side-chains of Val and Ile residues.[5] The hydrophobic fence created by these residues was thought to protect effectively the metal complex molecule against hydrolysis reactions. The side-chains of HmS are neither hydrophobic nor very bulky. The presence of four hydroxyl groups in HmS-HmS unit, however, could affect the complex stability due to a variety of interactions involving four alcoholic groups. In order to detect possible interactions we have applied 1-D and 2-D proton NMR techniques mainly

Table 1 Stability constants and spectroscopic characterization of complexes formed by H-HmS-HmS-His-OH and H-HmS-HmS-His-NH_2

Species	log β[a]	UV/VIS: λ/nm (ε/M^{-1} cm^{-1})	CD: λ/nm ($\Delta\varepsilon$/M^{-1} cm^{-1})
H-HmS-HmS-His-OH			
HL	7.140(1)		
H_2L	13.176(1)		
H_3L	15.848(2)		
NiL	4.7(1)		
$NiH_{-2}L$	−4.75(1)	420[b] (120)	412[b] (0.602)
	−14.6(1)		475[b] (−0.341)
$NiH_{-3}L$			
H-HmS-HmS-His-NH_2			
HL	6.636(3)		
H_2L	12.322(3)		
$NiH_{-2}L$	−4.13(8)	416[b] (130)	263[c] (0.870)
			411[b] (1.807)
			479[b] (−1.178)

[a] $\beta(NiH_iL) = [NiH_iL]/\{[Ni^{2+}][H^+]^i[L]\}$. Standard errors on the last digits are included in parentheses. [b] d–d Transition. [c] $N_{im}\rightarrow Ni^{II}$ and $N^-\rightarrow Ni^{II}$ CT transitions.

Table 2 (a) pK_{av} and log K* obtained for nickel(II) and copper(II) complexes according to the equations log K* = log $\beta(NiH_{-2}L)$ − log $\beta(H_2L)$ and $pK_{av} = (pK_{(NH2\text{-}X\text{-}Y\text{-}His)} + pK_{(NH2\text{-}Y\text{-}His\ or\ \text{-}Y\text{-}Gly)} + pK_{(NH2\text{-}His\ or\ \text{-}His\text{-}Gly)} + pK_{(NHimidazole\ (X\text{-}Y\text{-}His))})/4$

Ligand	pK_{av}	log K*
Nickel(II) complexes		
H-Gly-Gly-His-OH[a]	8.05	−21.78
H-Val-Ile-His-Asn[b]	7.51	−19.75
H-Arg-Tyr-His-Gly-Asn $_{HP2}$[c]	7.13	−19.23
H-HmS-HmS-His-OH[d]	7.37	−17.92
H-HmS-HmS-His-NH_2[d]	7.15	−16.45
Copper(II) complexes		
H-Gly-Gly-His-OH[a]	8.05	−16.40
H-Ser-Ser-His-OH[e]	7.64	−15.15
H-Ser-HmS-His-OH[e]	7.58	−14.12
H-HmS-Ser-His-OH[e]	7.45	−14.05
H-Arg-Tyr-His-Gly-Asn_{HP2}[c]	7.13	−14.24
H-HmS-HmS-His-OH[d]	7.37	−13.12
H-HmS-HmS-His-NH_2[d]	7.15	−11.04

(b) pK for amine and imidazole groups of the dipeptides used for the calculation of the pK_{av} values of the discussed peptides

Ligand	NH_2	N_{imid}
Ile-Gly[f]	8.07	
His-Gly[g]	7.59	5.94
Gly-His[g]	8.22	
His[h]	9.12	6.01
Tyr-His[i]	7.63	

[a] Ref. 24. [b] Ref. 5. [c] Ref. 6. [d] This work. [e] Unpublished data. [f] Ref. 25. [g] Ref. 26. [h] Ref. 27. [i] Ref. 28.

Table 3 The NMR parameters for the metal-free and nickel(II) complex (4N) of (a) H-HmS-HmS-His-OH and (b) H-HmS-HmS-His-NH_2

	β-$CH_{2\,his}$		α-CH_{his}	H-C4$_{im}$	H-C2$_{im}$	HmS CH_2 δ_A	δ_D	HmS CH_2 δ_B	δ_C	HmS CH_2 δ_E	δ_H	HmS CH_2 δ_F	δ_G
(a)													
δ	3.142	3.000	4.461	6.957	7.784	3.986	3.876	3.935	3.885	3.841	3.552	3.747	3.573
R_1/s^{-1}	1.927	1.906	0.408	0.237	0.185	1.725	1.815	1.762	1.790	1.633	1.605	1.606	1.626
$J_{H\text{-}H}$/Hz	15.0		4.7 7.7			12.0		12.0		12.0		12.0	
H-HmS-HmS-His-OH + Ni^{II}													
δ	3.056	2.845	4.038	6.876	7.493	4.068	3.546	3.970	3.681	3.829	3.530	3.820	3.574
R_1/s^{-1}	2.217	2.143	0.558	0.202	0.182	1.784	1.860	1.872	1.846	1.751	1.811	1.759	1.797
$J_{H\text{-}H}$/Hz	14.9		3.5 4.1			11.19		11.37		11.74		11.74	
H-HmS-HmS-His-OH oxidised + Ni^{II}													
δ	2.896	2.770	5.188	6.977	7.549								
(b)													
δ	3.165	2.987	4.576	6.984	7.690	3.963	3.883	3.878	3.853	3.799	3.563	3.782	3.555
R_1/s^{-1}	1.621	1.548	0.411	0.206	0.177	1.265	1.383		1.443	1.429	1.451	1.434	1.420
$J_{H\text{-}H}$/Hz	15		4.9 9.1			9.5		10		9.5		9.5	
HmS-HmS-His-NH_2 + Ni^{II}													
δ	3.127	2.854	4.206	6.920	7.540	4.107	3.564	4.080	3.524	3.852	3.591	3.798	3.543
R_1/s^{-1}	2.184	2.141	0.534	0.234	0.193				1.443		1.447	1.434	1.412
$J_{H\text{-}H}$/Hz	15.2		3.0 4.2			9.5		9.5		10		10	

ROESY spectra. Complete resonance assignment was obtained by TOCSY, NOESY and ROESY.

Metal-free ligands

Proton NMR spectra of H-HmS-HmS-His-OH performed at different pH and 2-D spectra allow us to assign the proton signals to the particular methyl protons of HmS residues (Table 3). The pH dependence of the chemical shifts of methylene protons of N-terminal HmS and imidazole ring protons can be used to calculate the protonation constants of N-terminal amine and imidazole nitrogens, respectively. Assuming that the pH dependence of the chemical shifts of imidazole ring protons depends mostly on protonation of imidazole nitrogens and those of N-terminal HmS methylene protons on protonation of the amine group, the protonation constants and the ionization microconstants were calculated (Table 4, Scheme 1). During

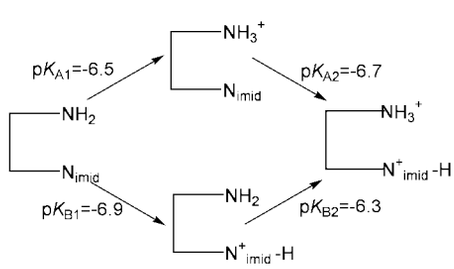

Scheme 1 Proton ionization scheme defining the microconstants calculated from the proton NMR and potentiometric data. Their values are also given.

deprotonation processes all chemical shifts of the HmS methylene protons are shifted upfield except that observed for the proton of the second HmS residue (proton A, Fig. 1). This unusual pH dependence could suggest a distinct peptide conformation change upon ligand deprotonation. Theoretical calculations performed for the metal-free peptide (see below) suggest hydrogen bond formation between the N-terminal amino group and the imidazole nitrogens in HL species. This hydrogen bond stabilizes the closed peptide conformation shown in Fig. 2(a). The ligand deprotonation HL $\longrightarrow$ L + H^+ breaks this bond and destabilizes the mentioned above conformation.

Table 4 The pK values (including isotopic effect of D_2O on the glass electrode, 0.4 unit, ref. 29) calculated by NMR measurements for the methylene group of HmS residues and imidazole H-C2 and H-C4 calculated for H-HmS-HmS-His-OH ligand

Protons		pK		pK
For NH_2 N-terminal				
H_A–C–H_D	A	6.31	D	6.42
H_B–C–H_C	B	5.98	C	6.42
H_E–C–H_H	E	6.45	H	6.56
H_F–C–H_G	F	6.50	G	6.46
For N_{im} imidazole				
H–C_{imid}	H-C2$_{im}$	6.88	H-C4$_{im}$	6.93

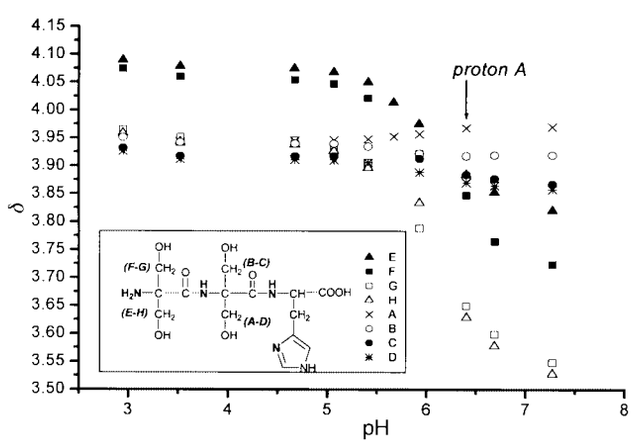

Fig. 1 pD Dependence of the chemical shifts of HmS methylene protons. Proton assignment is given in the insert.

Spin–lattice relaxation rates (R_1) of unexchangeable protons at pH 7, also reported in Table 3, show that the average R_1 values of N-terminal HmS protons are lower (1.62 s^{-1}) than those of the second HmS residue (1.77 s^{-1}). Since extreme narrowing conditions applied, the observed behaviour may support the more rigid structure of the N-terminal HmS residue involved in the hydrogen bond with imidazole nitrogen.

Table 5 (a) Calculated bond lengths (Å) in the terminal amino group and subsequent peptide bonds. In the case of N–H bonds, NBO bond populations are also given (2.0 is for a full single bond)

Bond	H-Gly-Gly-His-OH	H-HmS-HmS-His-OH
Terminal N–H	1.006/occ. 1.9897	1.022/occ. 1.9889
C=O	1.252	1.253
C–N	1.390	1.314
N–H	1.000/occ. 1.9825	1.008/occ. 1.9743
C=O	1.275	1.258
C–N	1.351	1.317
N–H	1.002/occ. 1.9824	0.996/occ. 1.9806

(b) Calculated atomic charges of N and carbonyl O atoms

Atom	H-Gly-Gly-His-OH	H-HmS-HmS-His-OH
(1) terminal N_{NH2}	−0.928	−0.940
(1) carbonyl O	−0.669	−0.604
(2) peptide N	−0.655	−0.634
(2) carbonyl O	−0.732	−0.634
(3) peptide N	−0.638	−0.630
(3) $N_{imidazole}$	−0.528	−0.537

The value in parentheses indicates the number of residues in the peptide chain.

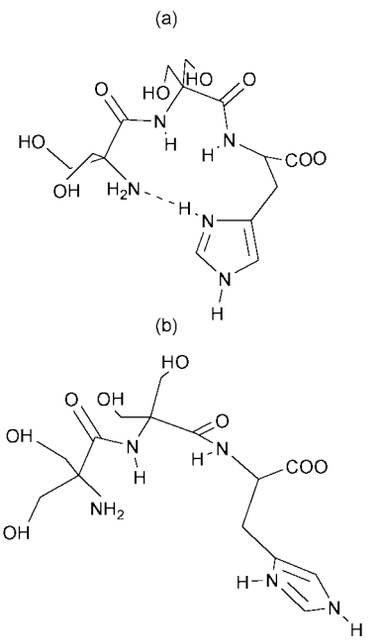

Fig. 2 Closed (a) and open (b) peptide conformation found for H-HmS-HmS-His-OH by theoretical calculations.

Theoretical calculation results

Owing to a significant conformational flexibility of the H-HmS-Hms-His-OH molecule, many structures corresponding to energetic local minima have been found. Of all these, however, the most stable are: closed-ring structure with proton transfer and resulting intramolecular hydrogen bond between the terminal NH_2 group and protonated imidazole moiety (Fig. 2a) and similar open ring structure without proton transfer (3.5 kcal mol^{-1} less stable, Fig. 2b). In case of H-Gly-Gly-His-OH the hydrogen-bonded closed-ring structure is also the energy minimum, but here the proton transfer does not occur (which is visible when larger basis sets are used; notably atoms involved in hydrogen bonding must have polarization functions). Further discussion is restricted to closed-ring structure, present also in the case of H-Gly-Gly-His-OH tripeptide. Table 5(a) shows the N–H, C–N and C=O distances of peptide bonds and N–H bond populations, and Table 5(b) NBO atomic charges for nitrogen and carbonyl oxygen atoms. Similarity of the conformations of the two considered tripeptides suggests that any significant changes of the geometrical parameters should be attributed to the electron-withdrawing potential of the side groups in the α-hydroxymethylserine residues. Lowering of N–H bond occupancies when comparing H-Hms-Hms-His-OH to H-Gly-Gly-His-OH tripeptide reflects an increase of proton acidity and weakening of these bonds. In fact, N–H bonds of the terminal amino group and the first amide bond are elongated in H-Hms-Hms-His-OH with respect to H-Gly-Gly-His-OH, whereas in the case of the second amide proton a shortening is actually observed in spite of a bond occupancy decrease (probably due to the conformational differences). Moreover, (O=)C–N(H) bonds, being of different lengths in H-Gly-Gly-His-OH, are in the modified tripeptide shortened and of equal length. This shortening is an obvious sign of π-electron density increase in the bond. Changes of 0.07–0.10e in carbonyl oxygen atom charges suggest that the electron density is partially withdrawn from these atoms.

The theoretical result suggesting that in monoprotonated HL species the protonation site is at imidazole nitrogen (lower pK value for amine nitrogen protonation) is rather striking. However, the protonation constants calculated from the proton NMR spectra (see above, Table 4, Scheme 1) seem to support this unusual finding.

Nickel(II) complexes

Potentiometric and spectroscopic data indicate formation of the complexes with the stabilities as shown in Table 1, Fig. 3(a). The stability constants of the other known X-Y-His peptide complexes are collected for comparison (Table 2a). As was found in the case of Cu^{II},[3] the HmS-HmS-His ligands are the most powerful chelators for Ni^{II}. The comparison of the 4N complexes in Table 2(a) clearly indicates the unusual gain in complex stability when two HmS residues are inserted at the N-terminal side of His. The competitive plot (Fig. 3b) comparing the binding ability of H-HmS-HmS-His-NH_2 and the other powerful ligand, the pentapeptide N-terminal fragment of human protamin HP2, shows that only a negligible amount of Ni^{II} binds to the latter peptide in 1 : 1 : 1 H-HmS-HmS-His-NH_2 : $HP2_{1\text{-}5}$: Ni^{II} solution.

The considerable increase in binding ability may derive among other factors from the direct or indirect interactions involving the side-chains of the particular residues.[17] The HmS-HmS dipeptide fragment contains four hydroxyl groups able to interact with metal ions or between each other. These interactions between the side-chains seem to affect the complex stability as suggested earlier for the metallopeptide complexes.

However, ROESY experiments (such as shown in Fig. 4) carried out at a mixing time of 300 ms only show the geminal, or Hα-Hβ, dipole–dipole connectivities, thus excluding the occurrence of any inter-side chain interactions.

All relaxation rates of HmS unexchangeable protons were found to be very close to each other (Table 3). Thus, similar local mobilities may be suggested for both HmS residues in the metal complex. It should be mentioned that, in the case of any dipole–dipole inter-side chain interaction, differences would be expected in the measured relaxation rates of the protons involved.

The other critical factor influencing the complex stability is the basicity of the bound nitrogens. Sigel and Martin[18] have shown that a N-terminal amino group has some impact on the stability of simple {N,O} complexes, while the effect of the basicity of a second amino group involved in amide bond formation is less evident. The lack of any impact of the inter-side chain interactions may indicate the metal-bound donor basicity is the only distinct parameter influencing the binding ability of the peptide molecule. In order to evaluate the basicity effect of the amine groups involved in the peptide bonds, the

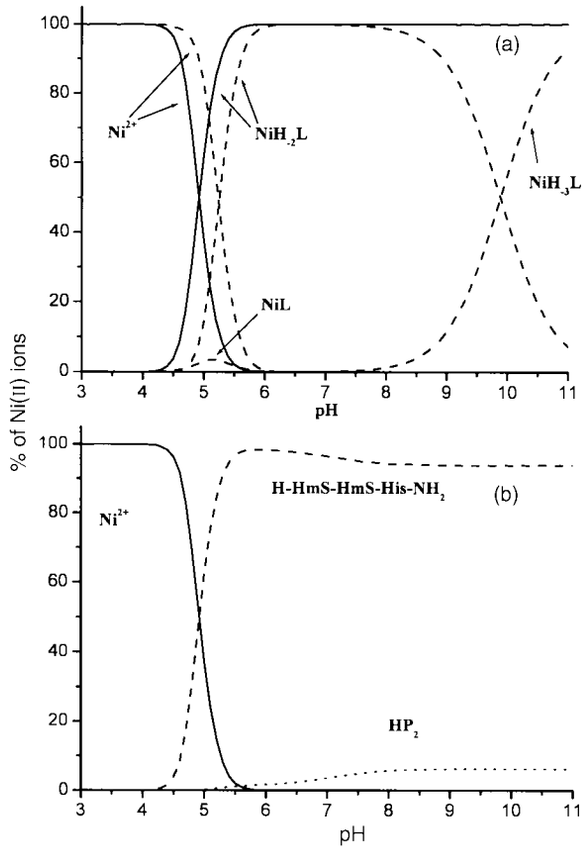

Fig. 3 The species distribution curves for equimolar Ni^{II}–H-HmS-HmS-His-OH (dashed line) and equimolar Ni^{II}–H-HmS-HmS-His-NH_2 (solid line) solutions for 10^{-3} M concentrations (a). The competitive plot of H-HmS-HmS-His-NH_2 and the human protamin HP2 in 1 : 1 : 1 H-Hms-HmS-His-NH_2: $HP2_{1\text{-}5}$: Ni^{II} solution for 10^{-3} M concentration (b).

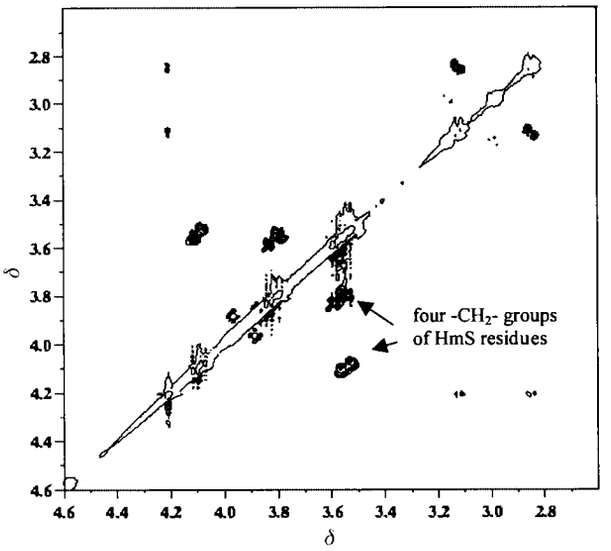

Fig. 4 The ROESY spectra with 36 hours acquisition time of the 4N complex Ni^{II}–H-HmS-HmS-His-NH_2 in the aliphatic region at pD 7.3.

relation between the log K^* and average pK value of imidazole and amino groups of the residues inserted in the peptide sequence (pK_{av}) was plotted (Table 2a,b; Fig. 5a,b). The pK values for the second residue in the tripeptide (and fourth in tripeptide amide) were assumed to be those found for its amine group with this residue at the first position in the dipeptide molecule. It should be mentioned here that the use of such an approach for Cu^{II}– and Ni^{II}–dipeptide systems to evaluate the amide nitrogen ability leads to rather complicated relations.[18,19]

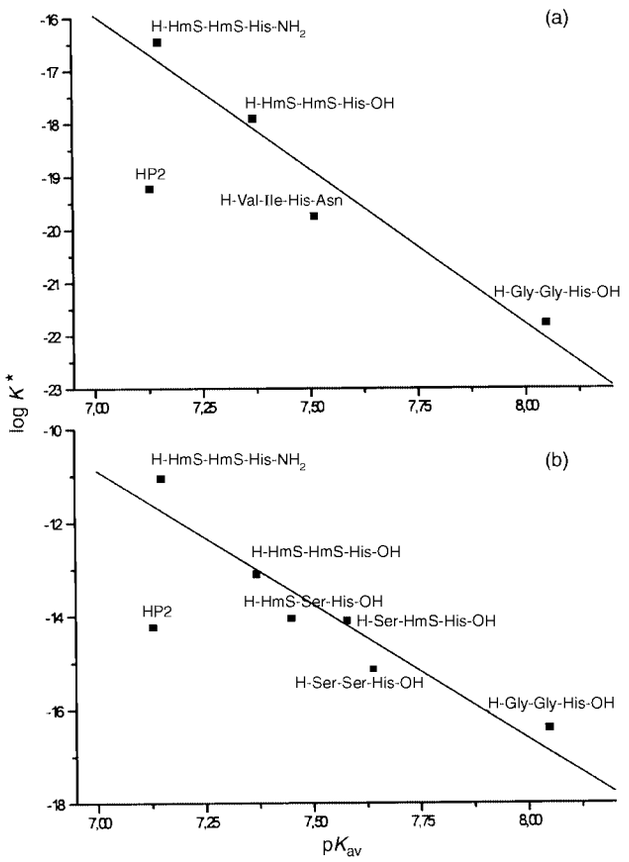

Fig. 5 The relation between log K^* and the amine group basicity expressed by the pK_{av} value of the amine groups of the residues inserted into the peptide sequence for nickel(II) (a) and copper(II) complexes (b).

The plots shown in Fig. 5 are rather surprising. The relations are almost linear and indicate that lower basicity of the amide nitrogen leads to higher stability of the complexes formed. The most striking is the fact that the log K^* value of highly hydrophobic H-Val-Ile-His-Asn peptide follows very closely the plotted relation. This could suggest only a minor effect of the hydrophobic amino acid side-chains on the complex stability. The other unusual finding is that higher basicity of the amine nitrogen results in its lower binding ability. The most effective amide nitrogens are those derived from the most acidic ammonium groups. A lower pK_{av} value makes the amide proton less competitive for metal ions and deprotonation with simultaneous amide nitrogen binding by metal ion occurs at lower pH; however its binding to metal ion should be more efficient when the amide nitrogen is more basic. The only ligand which does not follow the plotted relation, both for nickel(II) and copper(II) complexes, is the pentapeptide HP2 N-terminal fragment. The protamin pentapeptide having similar average value of "amine acidity" as HmS-HmS-His-NH_2 forms complexes about three orders weaker than the latter ligand. This discrepancy from the discussed relation can derive from the steric effects caused by the unbound residues of the distinctly longer HP2 ligand.

Theoretical calculations performed for H-Gly-Gly-His-OH and H-HmS-HmS-His-OH indicate that the involvement of the less basic amino nitrogen (HmS) in amide bond formation results in weakening of the N–H bond as expected (Table 5). The calculations also show, however, that in the case of the more acidic HmS nitrogen the formed carbon–nitrogen bond (in the amide group) is distinctly shorter than that of H-Gly-Gly-His-OH (Table 5a). The shortening of the (O=)C–N(H) bond indicates an increase of the π-electron contribution to this bond and likely the increase of π-electron contribution to the amide nitrogen–metal bond. The change in the amide nitrogen

acidity is also seen in the calculated atomic charges calculated on amine and amide nitrogens and carbonyl oxygens (Table 5b).

Oxidation of Ni^{II}–HmS-HmS-His-(OH) 4N complex

During the NMR measurements of the $NiH_{-2}L$ complex with tripeptide two sets of signals could be observed for the His protons. The major spectrum corresponds to the parent 4N complex with Ni^{II} bound to $\{NH_2,2N^-,N_{im}\}$ donor set. The two sets of proton spectra observed for the His residue strongly suggest that the minor complex has the same binding mode as the major one but some modification occurs at the His residue. The most likely seems to be oxidative decarboxylation catalysed by the co-ordinated Ni^{II} observed earlier for similar nickel complexes.[20,21] The likely structure of the oxidized nickel(II) complex is shown in Scheme 2. A detailed study on the oxidation mechanism is in progress.

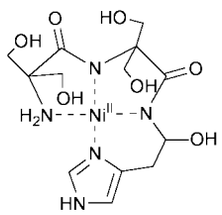

Scheme 2

Conclusion

Insertion of two α-hydroxymethylserine residues in the N-terminal albumin-like sequence leads to a most effective peptide chelating agent for copper(II) and nickel(II) ions. The metal-free ligand has two unexpected properties: (i) the N-terminal ammonium group is more acidic than the imidazole nitrogen and (ii) the hydrogen bond between the N-terminal amino group and imidazole ring nitrogen stabilizes the cyclic peptide structure. The latter feature predicted by theoretical calculations seems to support earlier experimental findings, which have shown that Cu^{II} or Ni^{II} may take the place of the proton between the above mentioned nitrogens forming a metal complex with similar cyclic structure.[22,23]

The very acidic ammonium group of the HmS residue changes distinctly the electron density within the amide bond causing the amide nitrogen to become a much more effective donor than the nitrogens derived from amino acids with more basic amino functions. The comparison of the complexes having different amino acid residues seems to indicate that hydrophobic residues can have a minor effect on the complex stability. However, the small number of available complexes for comparison make the latter conclusion rather tentative.

Acknowledgements

This work was supported by the Polish State Committee for Scientific Research (KBN 3T09A 105 14 and SPUB/COST/T-9/DZ 44/99 KBN 3T0959111V8). P. M. thanks COST action D8 for financial support. This work was performed within the D8 0018/97 project.

References

1 T. Kowalik-Jankowska, H. Kozłowski, M. Stasiak and M. T. Leplawy, *J. Coord. Chem.*, 1996, **40**, 113.
2 T. Kowalik-Jankowska, M. Stasiak, M. T. Leplawy and H. Kozłowski, *J. Inorg. Biochem.*, 1997, **66**, 193.
3 P. Młynarz, W. Bal, T. Kowalik-Jankowska, M. Stasiak, M. T. Leplawy and H. Kozłowski, *J. Chem. Soc.*, *Dalton Trans.*, 1999, 109.
4 P. Młynarz, T. Kowalik-Jankowska, M. Stasiak, M. T. Leplawy and H. Kozłowski, *J. Chem. Soc.*, *Dalton Trans.*, 1999, 3673.
5 W. Bal, G. N. Chmurny, B. D. Hilton, P. J. Sadler and A. Tucker, *J. Am. Chem. Soc.*, 1996, **118**, 4727.
6 W. Bal, M. Jeżowska-Bojczuk and K. S. Kasprzak, *Chem. Res. Toxicol.*, 1997, **10**, 906.
7 A. Bax and D. G. Davis, *J. Magn. Reson.*, 1985, **65**, 355.
8 A. A. Bothner-By, R. L. Stephens, J. T. Lee, C. D. Warren and R. W. Jeanloz, *J. Am. Chem. Soc.*, 1984, **106**, 111.
9 H. M. Irving, M. H. Miles and L. D. Pettit, *Anal. Chim. Acta*, 1967, **38**, 479.
10 P. Gans, A. Sabatini and A. Vacca, *J. Chem. Soc.*, *Dalton Trans.*, 1985, 1196.
11 M. Stasiak, W. M. Wolf and M. T. Leplawy, *J. Pept. Sci.*, 1998, **4**, 46.
12 M. Stasiak and M. T. Leplawy, *Lett. Pept. Sci.*, 1998, **5**, 449.
13 K. Barlos, O. Chatzi, D. Gatos and G. Stavropoulos, *Int. J. Pept. Protein Res.*, 1991, **37**, 513.
14 S. Miertus and J. Tomasi, *Chem. Phys.*, 1982, **65**, 239.
15 J. E. Carpenter and F. Weinhold, *J. Mol. Struct.* (*Theochem*), 1988, **169**, 41.
16 GAUSSIAN 94, Revision E.2, M. J. Frisch, G. W. Trucks, H. B. Schlegel, P. M. W. Gill, B. G. Johnson, M. A. Robb, J. R. Cheeseman, T. Keith, G. A. Petersson, J. A. Montgomery, K. Raghavachari, M. A. Al-Laham, V. G. Zakrzewski, J. V. Ortiz, J. B. Foresman, J. Cioslowski, B. B. Stefanov, A. Nanayakkara, M. Challacombe, C. Y. Peng, P. Y. Ayala, W. Chen, M. W. Wong, J. L. Andres, E. S. Replogle, R. Gomperts, R. L. Martin, D. J. X. Fox and J. S. Binkley, Gaussian Inc., Pittsburgh, PA, 1995.
17 H. Kozłowski, W. Bal, M. Dyba, T. Kowalik-Jankowska, *Coord. Chem. Rev.* 1999, **184**, 319.
18 H. Sigel and R. B. Martin, *Chem. Rev.*, 1982, **82**, 385.
19 R. B. Martin, in *Metal Ions in Biological Systems*, ed. H. Sigel, M. Decker, New York, 1987, vol. 23, p. 123.
20 W. Bal, M. I. Djuran, D. W. Margerum, E. T. Gray, Jr., M. A. Mazid, R. T. Tom, E. Nieboer and P. Sadler, *J. Chem Soc.*, *Chem. Commun.*, 1994, 1889.
21 T. Sakurai and A. Nakahara, *Inorg. Chim. Acta*, 1979, **34**, L243.
22 W. Bal, M. Jeżowska-Bojczuk, H. Kozłowski, L. Chrusciñski, G. Kupryszewski and B. Witczuk, *J. Inorg. Biochem.*, 1995, **57**, 235.
23 W. Bal, H. Kozlowski, R. Robbins and L. D. Pettit, *Inorg. Chim. Acta*, 1995, **231**, 7.
24 R. W. Hay, M. M. Hassan and Chen You-Quan, *J. Inorg. Biochem.*, 1993, **52**, 17.
25 H. Sigel, *Inorg. Chem.*, 1975, **14**, 1535.
26 I. Sovago, E. Farkas and A. Gargely, *J. Chem. Soc.*, *Dalton Trans.*, 1982, 2159.
27 H. Kozłowski, A. Anouor and T. Kowalik-Jankowska, *Inorg. Chim. Acta*, 1993, **207**, 223.
28 O. Yamauchi, K. Tsujie and A. Odani, *J. Am. Chem. Soc.*, 1985, **107**, 659.
29 W. U. Primose, in *NMR of Macromolecules*, ed. G. C. K. Roberts, Oxford University Press, Oxford, New York, Tokyo, 1993, p. 22.

Paper a909354k